nucl-th/9608012

Quasielastic K^+-nucleus scattering

A. De Pace
Istituto Nazionale di Fisica Nucleare, Sezione di Torino,
via P.Giuria 1, I-10125 Torino, Italy

C. García-Recio
Departamento de Física Moderna, Faculdad de Ciencias,
Universidad de Granada, E-18071 Granada, Spain

E. Oset
Departamento de Física Teórica and Instituto de Física Corpuscular,
Centro Mixto Universidad de Valencia – Consejo Superior de Investigaciones Científicas,
46100 Burjassot, Valencia, Spain
(August 1996)

Abstract

Quasielastic K^+-nucleus scattering data at $q = 290$, 390 and 480 MeV/c are analyzed in a finite nucleus continuum random phase approximation framework, using a density-dependent particle-hole interaction. The reaction mechanism is consistently treated according to Glauber theory, keeping up to two-step inelastic processes. A good description of the data is achieved, also providing a useful constraint on the strength of the effective particle-hole interaction in the scalar-isoscalar channel at intermediate momentum transfers. We find no evidence for the increase in the effective number of nucleons participating in the reaction which has been reported in the literature.

25.80.Nv, 25.70.Bc, 21.60.Jz

I. INTRODUCTION

Quasielastic studies are traditionally a good source of information about nuclear and nucleon structure. The main tool has been usually represented by electron scattering experiments, since in this case the elementary probe-nucleon reaction mechanism is regarded to be under better control. However, not all the possible nuclear response functions can be accessed in this way and, furthermore, the extraction from the data of the response functions that enter electron scattering can be model dependent.

Hadronic probes are an alternative source of quasielastic data. Among them it is particularly interesting the case of K^+-nucleus scattering, since, for kaon laboratory momenta below 800 MeV/c, the elementary K^+-nucleon (K^+N) interaction is much weaker than other hadron-nucleon interactions. In fact, a weaker elementary interaction allows the projectile to penetrate deeper inside the nucleus, thus probing regions of higher density and, consequently, being more sensitive to collective phenomena.

Such an experiment has been performed at BNL, where quasielastic K^+-nucleus double-differential cross sections have been measured for kaons with a laboratory momentum of 705 MeV/c, using D, C, Ca and Pb as targets [1,2]. Data have been taken for scattering at 24°, 34° and 43°, corresponding to approximately fixed momentum transfers of 290, 390 and 480 MeV/c. In the case of C, the data have been taken for all the momenta, whereas for Ca and Pb they are available at 290 and 480 MeV/c.

In Refs. [1,2] the data have been analyzed using various relativistic models to describe the nuclear dynamics; on the other hand, the distortion of the incoming kaons has been accounted for employing a very simple model, based on the effective number of nucleons participating in the reaction, $N_{\rm eff}$ (see Sec. II D). The "experimental" values found for $N_{\rm eff}$ are $\sim 30\%$ higher than the ones calculated in the Glauber theory. This finding is rather puzzling, also in view of the fact that multiple scattering theory underestimates the nuclear elastic scattering data [3,4], a fact which has been interpreted as a signal of an enhancement of the in-medium K^+N cross section. As also noted in Ref. [2], the quasielastic cross section is, in general, proportional to the elementary single differential K^+N cross section and to the effective number of participating nucleons, the latter depending, in turn, on the total K^+N cross section (see Sec. II D for details). At the energy of the experiment, K^+N scattering is nearly isotropic, so that the differential and total cross sections are proportional; however, an increase in the K^+N cross section reduces $N_{\rm eff}$ (and viceversa), leaving a quasielastic cross section little dependent on the input K^+N amplitudes. Thus, the quasifree experiment on the one side does not shed light on the elastic scattering data and, on the other, it seems to pose another puzzling problem.

In this paper we would like to reanalyze the K^+-nucleus quasielastic data, using a more realistic model for the reaction mechanism, — already applied to (p,p') and (p,n) quasifree scattering [5,6], — based on a consistent implementation of Glauber theory for quasifree scattering. The nuclear dynamics has been treated through a finite nucleus continuum random phase approximation (RPA) calculation, also accounting for the coupling of the particle-hole (ph) states to higher order configurations (spreading width). The dynamics is non-relativistic, but the correct relativistic kinematics has been used.

We will show that the puzzling experimental outcome for $N_{\rm eff}$ is very likely an artifact of the naive fitting procedure employed in the analysis of the data and that a realistic (and

without free parameters) theoretical framework has no difficulties in giving a rather accurate description of the experimental cross sections.

In Sec. II we introduce the theoretical methods employed in the calculations: Here, one can find a brief description of the quasielastic nuclear responses in finite nuclei; of the RPA using density-dependent interactions; of the specific model for the ph effective potential that we have used; and of the response functions to hadronic probes up to two-step processes in the Glauber framework. In Sec. III, we display the results of our calculations and in the last Section we discuss their implications for the interpretation of the data.

II. THEORETICAL METHODS

A. Quasielastic nuclear response

The nuclear response function to an external probe, transferring momentum q and energy ω, is proportional to the imaginary part of the polarization propagator [7]:

$$R_\alpha(q,\omega) = -\frac{1}{\pi}\mathrm{Im}\Pi_\alpha(\boldsymbol{q},\boldsymbol{q};\omega) \ . \tag{2.1}$$

The latter reads

$$\begin{aligned}\Pi_\alpha(\boldsymbol{q},\boldsymbol{q}';\omega) = \sum_{n\neq 0}\langle\psi_0|\hat{O}_\alpha(\boldsymbol{q})|\psi_n\rangle\langle\psi_n|\hat{O}^\dagger_\alpha(\boldsymbol{q}')|\psi_0\rangle \\ \times\left[\frac{1}{\hbar\omega-(E_n-E_0)+i\eta}\right. \\ \left.-\frac{1}{\hbar\omega+(E_n-E_0)-i\eta}\right] \ ,\end{aligned} \tag{2.2}$$

where $\{|\psi_n\rangle\}$ is a complete set of nuclear eigenstates of energy E_n, $\hat{O}_\alpha(\boldsymbol{q})$ the second quantized expression of the vertex operator and α labels the spin-isospin channel. In the following, for the purpose of illustration, we shall deal explicitly only with the scalar-isoscalar channel, — which is, by the way, the dominant one in K^+N scattering at the energies of concern to us, — where $O(\boldsymbol{q},\boldsymbol{r}) = \exp(i\boldsymbol{q}\cdot\boldsymbol{r})$: The case of the spin modes, which is slightly complicated by the spin algebra, is treated in detail in Ref. [5].

The angular part of $\Pi(\boldsymbol{q},\boldsymbol{q}';\omega)$ (we now drop, for simplicity, the channel label α) can be handled through a multipole decomposition that reads

$$\Pi(\boldsymbol{q},\boldsymbol{q}';\omega) = \sum_{JM}\Pi_J(q,q';\omega)Y^*_{JM}(\hat{\boldsymbol{q}})Y_{JM}(\hat{\boldsymbol{q}}') \ , \tag{2.3}$$

so that

$$R(q,\omega) = -\frac{1}{4\pi^2}\mathrm{Im}\sum_J(2J+1)\Pi_J(\boldsymbol{q},\boldsymbol{q};\omega) \ . \tag{2.4}$$

In a mean field (shell model) framework, one has for the particle-hole (ph) polarization propagator:

$$\Pi^0_J(q,q';\omega) = \sum_{ph} Q^{JJ0}_{ph}(q) \left[\frac{1}{\omega - (\epsilon_p - \epsilon_h) + i\eta} - \frac{1}{\omega + (\epsilon_p - \epsilon_h) - i\eta} \right] Q^{JJ0^*}_{ph}(q') \ , \qquad (2.5)$$

where p (h) labels a complete set of single particle (hole) quantum numbers and

$$Q^{J\ell\sigma}_{ph}(q) = \langle j_p j_h; J|\ell\sigma; J\rangle (-i)^{\ell+1}(-1)^{\ell_h} 2[4\pi(2\ell_p+1)(2\ell_h+1)]^{1/2} \mathcal{I}_{\ell,ph}(q) \begin{pmatrix} \ell_p & \ell_h & \ell \\ 0 & 0 & 0 \end{pmatrix} \ . \qquad (2.6)$$

In (2.6), $\langle j_p j_h; J|\ell\sigma; J\rangle$ is the standard $LS - jj$ recoupling coefficient and

$$\mathcal{I}_{\ell,ph}(q) = \int_0^\infty dr\, r^2 j_\ell(qr) R_p(r) R_h(r) \ , \qquad (2.7)$$

$R_{p(h)}(r)$ being the radial particle (hole) wave function and $\epsilon_{p(h)}$ the associated eigenvalues. They are obtained by solving the Schroedinger equation with the Woods-Saxon potential

$$W(r) = \frac{W_0}{1 + e^{(r-R)/a}} + \left[\frac{\hbar c}{m_\pi^2 c^2} \right]^2 \frac{W_{so}}{ar} \frac{e^{(r-R)/a}}{\left[1 + e^{(r-R)/a}\right]^2} \boldsymbol{\ell} \cdot \boldsymbol{\sigma} \qquad (2.8)$$

(neglecting, for simplicity, the Coulomb term), where m_π is the pion mass and the following set of parameters has been employed:

$$\begin{array}{rcl@{\qquad}rcl} W_0 & = & -54.8\,\mathrm{MeV}, & W_{so} & = & -10\,\mathrm{MeV} \ , \\ R & = & 1.27\,A^{1/2}\,\mathrm{fm}, & a & = & 0.67\,\mathrm{fm} \ . \end{array} \qquad (2.9)$$

Note that the sum appearing in Eq. (2.5) should be understood as a sum over the discrete part of the spectrum and an integration over the continuum one. Indeed, contrary to the widespread procedure of calculating the polarization propagator in coordinate space and then Fourier transform to momentum space, we have directly evaluated Eq. (2.5) in the latter. Besides being fast and reliable, this procedure allows also for an important extension to the shell model polarization propagator, namely the inclusion of the *spreading width* of the ph states.

This can be accomplished by adding in Eq. (2.5) a complex ph self-energy, i. e. through the following substitution:

$$(\epsilon_p - \epsilon_h) \to (\epsilon_p - \epsilon_h) - \Sigma_{ph}(\omega) \ . \qquad (2.10)$$

Although Σ_{ph} could in principle be calculated, we shall actually employ a phenomenological parameterization, writing

$$\Sigma_{ph}(\omega) = \Delta_{ph}(\omega) + i\frac{\Gamma_{ph}(\omega)}{2} \ , \qquad (2.11)$$

with

$$\begin{aligned} \Gamma_{ph}(\omega) &= [\gamma_p(\hbar\omega + \epsilon_h) + \gamma_h(\epsilon_p - \hbar\omega)](1 + C_{TS}) \\ \Delta_{ph}(\omega) &= [\Delta_p(\hbar\omega + \epsilon_h) + \Delta_h(\epsilon_p - \hbar\omega)](1 + C_{TS}) \ . \end{aligned} \qquad (2.12)$$

The arguments of the functions $\gamma_{p(h)}$ and $\Delta_{p(h)}$ have been inferred from the analysis of the second order particle and hole self-energy contributions to Σ_{ph}. The coefficients C_{TS} represent the corrections, in each isospin T–spin S channel, due to the ph interference diagrams: These have been estimated [8] to contribute around 5% in $S = T = 1$ and $\approx 20 \div 25\%$ in $S = 0$, $T = 1$ and $S = 1$, $T = 0$; given the smooth dependence of the quasielastic response on the ph self-energy and the small contribution of these modes to the K^+-nucleus cross section, these corrections are not important and we shall set for simplicity $C_{TS} = 0$ in these channels. Concerning the channel $S = T = 0$, the estimate of Ref. [8] gives $C_{00} = -1$, resulting in a complete cancellation of the ph spreading width. This outcome is valid in nuclear matter and in the limit of very large angular momenta, which is presumably good in the quasielastic peak (QEP) region. However, at low transferred momenta the region of small energy transfers of the quasielastic response is dominated by resonances associated to specific (low) angular momenta. In that case it is a better approximation to retain the full width and, accordingly, we shall choose $C_{00} = -1 + \exp[-(\omega/\omega_0)^2]$ with $\omega_0 = 30$ MeV: Then, resonances in the $10 \div 20$ MeV range get a width of a few MeV, whereas for $\omega \gtrsim 30$ MeV there is essentially no spreading.

Finally, the $\gamma_{p(h)}$ are chosen according to the parametrization of Ref. [8], namely

$$\begin{aligned} \gamma_p(\epsilon) &= 2\alpha \left(\frac{\epsilon^2}{\epsilon^2 + \epsilon_0^2} \right) \left(\frac{\epsilon_1^2}{\epsilon^2 + \epsilon_1^2} \right) \theta(\epsilon) \\ \gamma_h(\epsilon) &= \gamma_p(-\epsilon) \ , \end{aligned} \tag{2.13}$$

symmetrical with respect to the Fermi energy ($\epsilon_F = 0$), which gives a reasonable fit of the particle widths for medium-heavy nuclei, using $\alpha = 10.75$ MeV, $\epsilon_0 = 18$ MeV and $\epsilon_1 = 110$ MeV [9]. The corresponding real parts are obtained through a once-subtracted dispersion relation [5].

A final remark, concerning relativistic kinematics effects on the response functions, is in order. We shall be concerned with momentum transfers up to 500 MeV/c, where purely kinematical relativistic effects are starting to be sizable. At $q = 500$ MeV/c the relativistic position of the QEP is ≈ 8 MeV below the non-relativistic one, the effect being even larger for energies on the right hand side of the QEP. In Ref. [10], it had been shown that the non-relativistic Fermi gas can be mapped into the relativistic one through the simple prescription

$$\omega \to \omega \left(1 + \frac{\omega}{2m_N} \right) \ . \tag{2.14}$$

The validity of (2.14) in a finite nucleus shell-model calculation has been checked in Ref. [11]. The main effect of properly accounting for the relativistic dispersion relation turns out to be a moderate shrink of the response functions at the right of the QEP (see Sec. III).

B. RPA with density-dependent interactions

The polarization propagator introduced in the previous subsection is used in this paper as input in a continuum RPA calculation of the response functions.

For a central density-independent interaction one has to solve, for each multipole J, the following integral equation (see Ref. [12] for the complications introduced by the tensor interaction):

$$\Pi_J^{\rm RPA}(q,q';\omega) = \Pi_J^0(q,q';\omega) + \frac{1}{(2\pi)^3}\int_0^\infty dk\, k^2 \Pi_J^0(q,k;\omega) V(k) \Pi_J^{\rm RPA}(k,q';\omega) \ , \tag{2.15}$$

$V(k)$ being the Fourier transform of the two-body potential. However, realistic effective nuclear interactions are in general density-dependent, especially in the scalar channels.

For a general interaction potential $V(\boldsymbol{r},\boldsymbol{r}')$, one can introduce the double Fourier transform

$$\begin{aligned} V(\boldsymbol{k},\boldsymbol{k}') &= \int d\boldsymbol{r}\, d\boldsymbol{r}'\, e^{-i\boldsymbol{k}\cdot\boldsymbol{r}} e^{i\boldsymbol{k}'\cdot\boldsymbol{r}'} V(\boldsymbol{r},\boldsymbol{r}') \\ &= \sum_J V_J(k,k')\, Y_{JM}(\hat{\boldsymbol{k}}) Y^*_{JM}(\hat{\boldsymbol{k}}') \ . \end{aligned} \tag{2.16}$$

Then, instead of Eq. (2.15), one has to solve the following RPA equations:

$$\begin{aligned} \Pi_J^{\rm RPA}(q,q';\omega) &= \Pi_J^0(q,q';\omega) + \frac{1}{(2\pi)^6}\int_0^\infty dk\, k^2 \int_0^\infty dk'\, k'^2\, \Pi_J^0(q,k;\omega) V_K(k,k') \Pi_J^{\rm RPA}(k',q';\omega) \\ &= \Pi_J^0(q,q';\omega) + \frac{1}{(2\pi)^3}\int_0^\infty dk'\, k'^2 K_J(q,k';\omega) \Pi_J^{\rm RPA}(k',q';\omega) \ , \end{aligned} \tag{2.17}$$

having defined the kernel

$$K_J(q,k';\omega) = \frac{1}{(2\pi)^3}\int_0^\infty dk\, k^2 \Pi_J^0(q,k;\omega) V_J(k,k') \ . \tag{2.18}$$

Clearly, in the case $V(\boldsymbol{r},\boldsymbol{r}') \equiv V(\boldsymbol{r}-\boldsymbol{r}')$ one has $V_J(k,k') = (2\pi)^3 V(k)\delta(k-k')/k^2$: The kernel (2.18) is then reduced to $K_J(q,k';\omega) = \Pi_J^0(q,k';\omega)V(k')$ and one gets back to Eq. (2.15).

From Eq. (2.17) it is apparent that the solution of the RPA equations with density-dependent forces does not pose any additional technical problem, apart from the input kernel, whose calculation is more involved.

As discussed in detail in the next subsection, in the calculations of Sec. III we have been using a parameterization of the effective nuclear interaction linear in the density. In general, in any (non-tensor) channel one has

$$\begin{aligned} V(\boldsymbol{r}_1,\boldsymbol{r}_2) &= V^{\rm ex}(\boldsymbol{r}_1-\boldsymbol{r}_2) + V^\rho(\boldsymbol{r}_1-\boldsymbol{r}_2)\, \widetilde{\rho}\left(\frac{\boldsymbol{r}_1+\boldsymbol{r}_2}{2}\right) \\ &\equiv V^{\rm ex}(r) + V^\rho(r)\, \widetilde{\rho}(R) \ , \end{aligned} \tag{2.19}$$

with $\boldsymbol{r} = \boldsymbol{r}_1 - \boldsymbol{r}_2$, $\boldsymbol{R} = (\boldsymbol{r}_1+\boldsymbol{r}_2)/2$ and $\widetilde{\rho}(R) = \rho(R)/\rho(0)$, $\rho(R)$ representing the nuclear density, here approximated by the standard Fermi distribution.

In momentum space (2.19) reads

$$V(\boldsymbol{k},\boldsymbol{k}') = V^{\rm ex}(k)(2\pi)^3\delta(\boldsymbol{k}-\boldsymbol{k}') + V^\rho\left(\frac{\boldsymbol{k}+\boldsymbol{k}'}{2}\right)\widetilde{\rho}(\boldsymbol{k}-\boldsymbol{k}') \tag{2.20}$$

and its Jth component in the angular momentum expansion (2.16) turns out to be

$$V_J(k,k') = V^{\rm ex}(k)\frac{(2\pi)^3}{k^2}\delta(k-k') + V_J^\rho(k,k') \tag{2.21}$$

where

$$V_J^\rho(k,k') = 2\pi \int d(\hat{\boldsymbol{k}}\cdot\hat{\boldsymbol{k}}')\, V^\rho\left(\frac{\boldsymbol{k}+\boldsymbol{k}'}{2}\right)\tilde{\rho}(\boldsymbol{k}-\boldsymbol{k}')P_J(\hat{\boldsymbol{k}}\cdot\hat{\boldsymbol{k}}')\ , \tag{2.22}$$

P_J representing the ordinary Legendre polinomials.

C. Effective ph interaction

Two strategies are possible in order to determine the effective ph interaction in the nuclear medium: One can either directly fix an effective potential by fitting some phenomenological properties or start with a bare nucleon-nucleon interaction and calculate the related G-matrix. Parameterizations of the ph interaction based upon the first procedure are generally only available at very low momentum transfers (in terms of Migdal-Landau parameters); since we are probing relatively high momenta, we have resorted to use a G-matrix and we have chosen the calculation of Ref. [13], which, in our view, has the following appealing features: It is based upon a realistic boson exchange potential; (nonlocal) exchange contributions are included in the effective interaction, which is conveniently parameterized in terms of Yukawa functions; a parameterization of the density dependence is also provided.

The potential is given using the standard representation in spin and isospin (no spin-orbit contribution will be considered in the following):

$$\begin{aligned} V(\boldsymbol{k}_f,\boldsymbol{k}_i;k_F) = {} & F + F'\boldsymbol{\tau}_1\cdot\boldsymbol{\tau}_2 + G\boldsymbol{\sigma}_1\cdot\boldsymbol{\sigma}_2 + G'\boldsymbol{\sigma}_1\cdot\boldsymbol{\sigma}_2\ \boldsymbol{\tau}_1\cdot\boldsymbol{\tau}_2 \\ & + TS_{12}(\hat{\boldsymbol{q}}) + T'S_{12}(\hat{\boldsymbol{q}})\boldsymbol{\tau}_1\cdot\boldsymbol{\tau}_2 + HS_{12}(\hat{\boldsymbol{Q}}) + H'S_{12}(\hat{\boldsymbol{Q}})\boldsymbol{\tau}_1\cdot\boldsymbol{\tau}_2\ , \end{aligned} \tag{2.23}$$

where $\boldsymbol{q} = \boldsymbol{k}_i - \boldsymbol{k}_f$, $\boldsymbol{Q} = \boldsymbol{k}_i + \boldsymbol{k}_f$ ($\boldsymbol{k}_i$, $\boldsymbol{k}_f$ being the relative momenta in the initial and final state, respectively) and the coefficients are density and momentum dependent.

However, before utilizing the nuclear matter interaction of Ref. [13] in a finite nucleus calculation of quasielastic responses, a few issues have to be addressed.

a) The density dependence of the G-matrix is given in terms of density dependent coupling constants, which is not very useful for our purposes. Furthermore, the parameterization is fitted for $0.95\text{fm}^{-1} < k_F < 1.36\text{fm}^{-1}$, k_F being the Fermi momentum, which spans a range of densities down to roughly 1/3 of the central density: Extrapolation of their parameterization to lower densities gives unreasonable results. Thus, we have chosen to employ the linear ρ dependence of Eq. (2.19) [or (2.20)], which is known to provide a reasonable parameterization (see, e. g., Ref. [14]). One can see in Fig. 1 a comparison of the two parameterizations for the k_F dependence of the effective interaction. It should be noted that most of the contribution to the quasielastic responses comes from densities where the two descriptions differ by a few per cent.

b) In order to obtain, at a fixed density, a local interaction, one can use the relation between q, Q and k_i, i. e., $Q = \sqrt{4k_i^2 - q^2}$, substituting k_i with a suitably chosen average

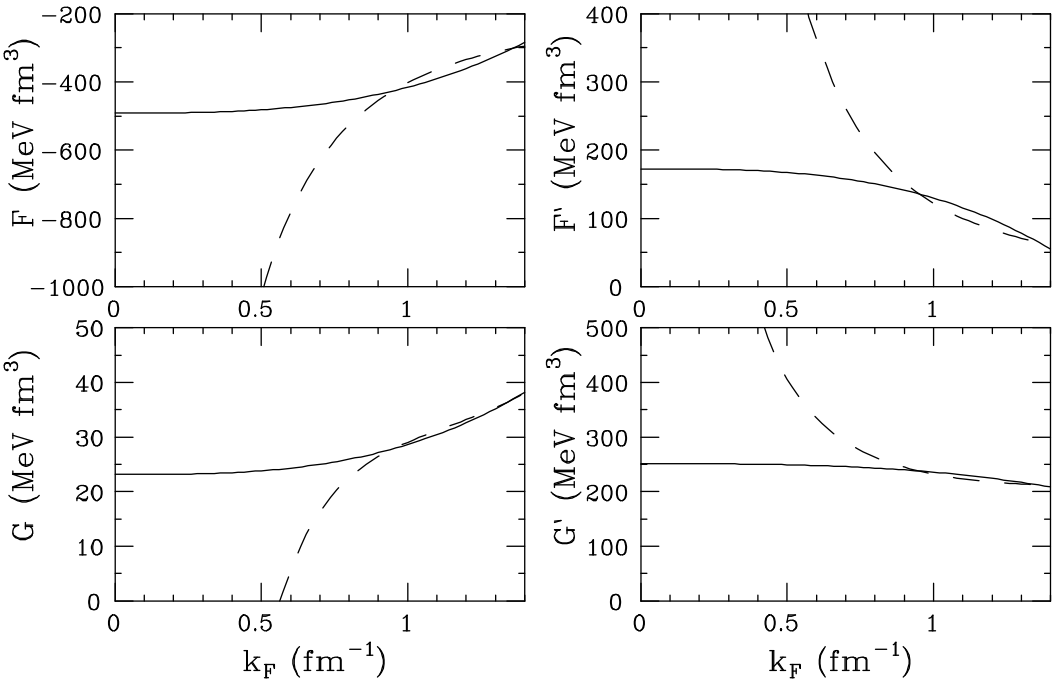

FIG. 1. Effective interaction in the non-tensor channels as a function of k_F at $q = 0$; linear (solid) and from Ref. [13] (dashed) density dependence.

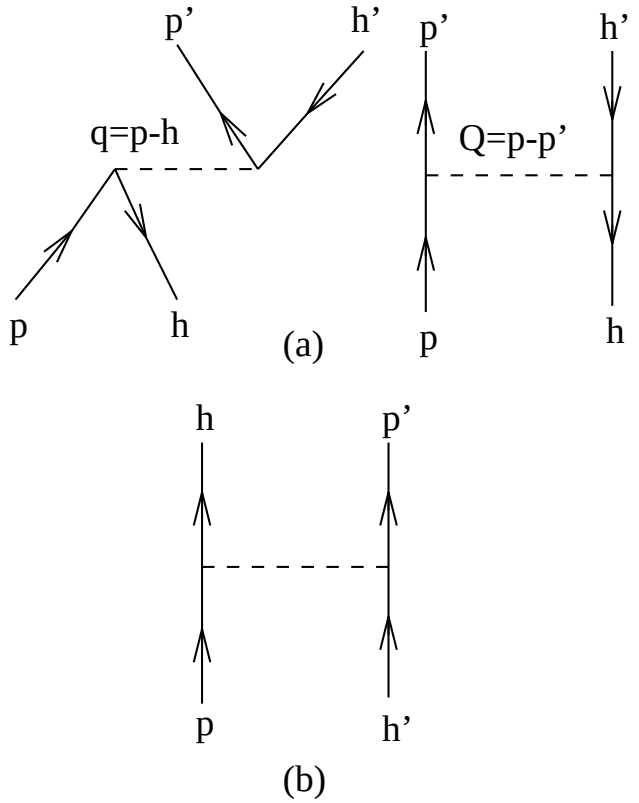

FIG. 2. (a) Direct and exchange ph matrix elements; (b) direct pp matrix element.

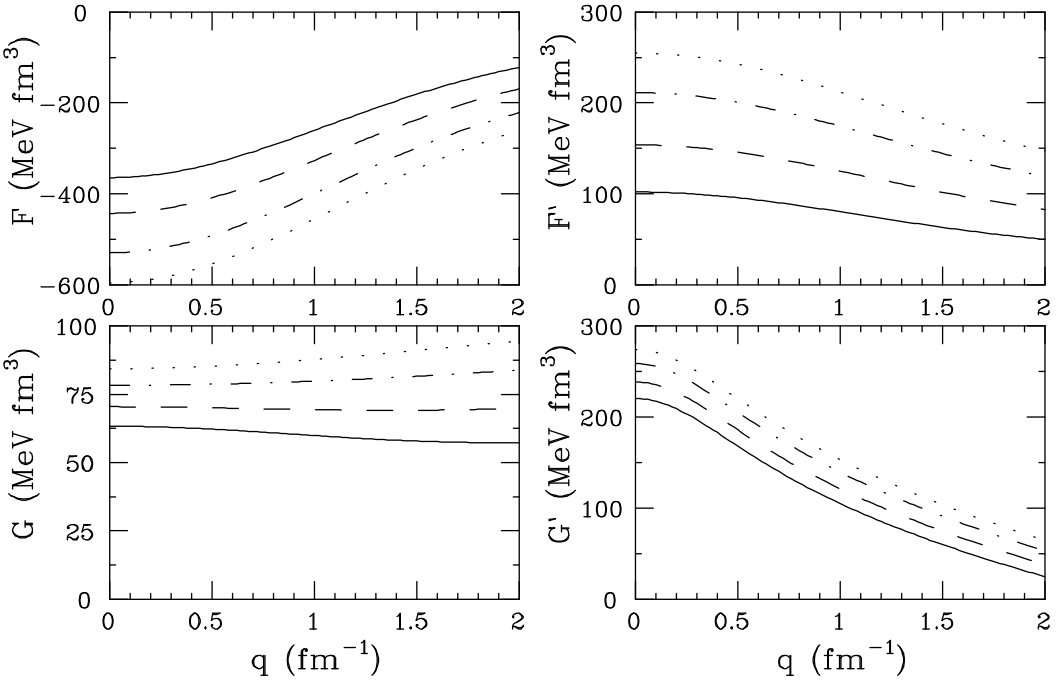

FIG. 3. Effective ph interaction in the non-tensor channels as a function of q at $k_F = 1.36$ (solid), 1.25 (dashed), 1.10 (dot-dashed) and 0.95 fm^{-1} (dotted).

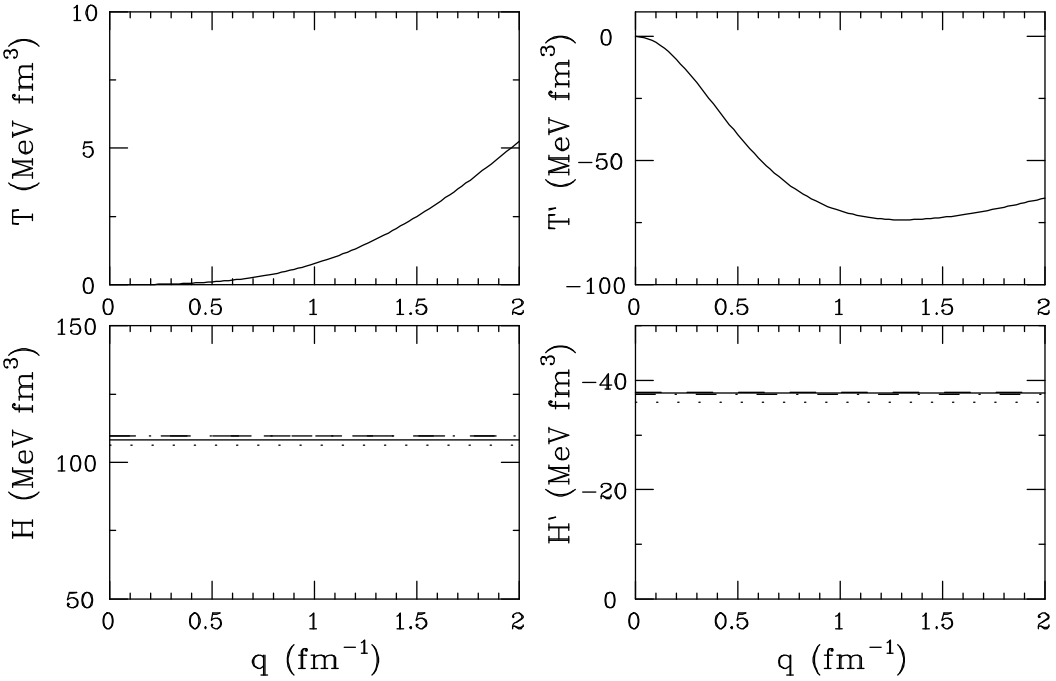

FIG. 4. As in Fig. 3, but for the tensor channels; T and T' do not depend on the density.

value, $\langle k_i \rangle$; then, the only independent momentum is q. The authors of Ref. [13] were interested in a potential for nuclear structure calculations: Hence, they put the momenta of the two nucleons in the initial state on the Fermi surface and averaged over the relative angle, getting $\langle k_i \rangle \approx 0.7 k_F$. Clearly, in this case one has the constraint $0 < q \lesssim 1.4 k_F$. On the other hand, we are interested in the ph interaction in the quasielastic region: One nucleon in the initial state is below the Fermi sea, while the other can be well above it. A look at Fig. 2 shows that $\boldsymbol{k}_i$ is defined, in terms of the particle and hole momenta, as $\boldsymbol{k}_i = (\boldsymbol{p} - \boldsymbol{h}')/2 = (\boldsymbol{h} - \boldsymbol{h}' + \boldsymbol{q})/2$. Thus, at fixed $\boldsymbol{q}$ one should average k_i over $\boldsymbol{h}$ and $\boldsymbol{h}'$, getting $\langle k_i \rangle \approx \sqrt{6k_F^2/5 + q^2}/2$. Now k_i is growing with q, so that there are no longer constraints on q, and the exchange momentum turns out to be constant, $Q = \sqrt{6/5} k_F$. One can see in Fig. 3 the resulting interaction in the non tensor channels.

c) In the case of the tensor channels things are simpler, since in the parameterization of Ref. [13] there is no explicit density dependence (Fig. 4). The coefficients of the exchange tensor operator, H and H', display a very mild density dependence, induced by Q, which is completely negligible. The only catch concerns the treatment of $S_{12}(\boldsymbol{Q})$: Assuming that $\boldsymbol{q}$ and $\boldsymbol{Q}$ are orthogonal, with some algebra one can show that $S_{12}(\hat{\boldsymbol{Q}}) = -S_{12}(\hat{\boldsymbol{q}})/2$. Note, however, that $80 \div 90\%$ of the quasielastic cross section for K^+ scattering is due to the scalar-isoscalar channel.

D. Response functions with hadronic probes

The formalism introduced above is not enough when one is dealing with strongly interacting probes, in which case a framework for the reaction mechanism must be provided. For this purpose, we have chosen the Glauber approach [15], including up to two-step inelastic processes.

Simple treatments within the Glauber theory usually amount to including the effects due to rescattering in an effective number of nucleons participating in the reaction, thus effectively renormalizing the response functions defined above. In the case of K^+ quasielastic scattering, this approach has been followed in Refs. [1,2,16].

However, a consistent treatment within Glauber theory leads one to the definition of *surface response functions* [5]. A detailed derivation, in particular for the spin-isospin channel, can be found in Ref. [5]. Here, we briefly sketch the relevant points, again using the scalar-isoscalar channel as example.

A surface polarization propagator can be obtained from (2.2) by substituting the vertex operator $O_\alpha(\boldsymbol{q}, \boldsymbol{r})$, which describes the probe-nucleon coupling, with

$$\begin{aligned} O_\alpha^{\rm surf}(\boldsymbol{q}, \boldsymbol{r}) = & \frac{1}{(2\pi)^2 f_\alpha(q)} \\ & \times \int d\boldsymbol{b}\, d\boldsymbol{\lambda}\, e^{-\widetilde{\sigma}_{\rm tot} T(b)/2} e^{i(\boldsymbol{q}-\boldsymbol{\lambda})\cdot\boldsymbol{b}} f_\alpha(\lambda) \\ & \times O_\alpha(\boldsymbol{\lambda}, \boldsymbol{r}) \ , \end{aligned} \tag{2.24}$$

$\boldsymbol{b}$ and $\boldsymbol{\lambda}$ being bidimensional vectors in the plane orthogonal to the direction of motion of the projectile, f_α the elementary probe-nucleon amplitudes, $\widetilde{\sigma}_{\rm tot}$ the effective total probe-nucleon cross section and

$$T(b) = \int_{-\infty}^{+\infty} dz\, \rho(r = \sqrt{b^2 + z^2}) \ , \tag{2.25}$$

$\rho(r)$ being the nuclear density. With these definitions, the effective number of participating nucleons is given as

$$N_{\rm eff} = \int d\boldsymbol{b}\, T(b) e^{-\widetilde{\sigma}_{\rm tot} T(b)} \ . \tag{2.26}$$

$\widetilde{\sigma}_{\rm tot}$ depends on the energy and we shall take the average over the total cross sections at the incoming and outgoing projectile energies: For K^+ scattering at $k = 705$ MeV/c, the variation of $\widetilde{\sigma}_{\rm tot}$ is rather weak, going roughly from 14 mb to 13 mb for energy losses up to 250 MeV.

One then finds, for the J-th multipole,

$$\begin{aligned}\Pi^{\rm surf}_{J(\alpha)}(q,q;\omega) = {} & \Pi_{J(\alpha)}(q,q;\omega) \\ & + \frac{1}{|f_\alpha(q)|^2} \int_0^\infty d\lambda\, \lambda \int_0^\infty d\lambda'\, \lambda'\, {\rm Re}[f^*_\alpha(\lambda)\, f_\alpha(\lambda')\, G^{(0)}_J(\lambda,\lambda';q)] \Pi_{J(\alpha)}(\lambda,\lambda';\omega) \\ & - 2 \frac{1}{|f_\alpha(q)|^2} \int_0^\infty d\lambda\, \lambda\, {\rm Re}[f^*_\alpha(q)\, f_\alpha(\lambda)\, H^{(0)}_J(\lambda;q)] \Pi_{J(\alpha)}(q,\lambda;\omega) \ , \end{aligned} \tag{2.27}$$

having set

$$G^{(0)}_J(\lambda,\lambda';q) = \sum_m c_{Jm} g^*_m(\lambda,q) g_m(\lambda',q) \tag{2.28a}$$

$$H^{(0)}_J(\lambda;q) = \sum_m c_{Jm} g_m(\lambda,q) \ , \tag{2.28b}$$

where

$$g_m(\lambda,q) = \int_0^\infty db\, b \left[1 - e^{-\widetilde{\sigma}_{\rm tot} T(b)/2}\right] J_m(\lambda b)\, J_m(qb) \tag{2.29}$$

and

$$c_{Jm} = I_{J+m} \frac{(J-m-1)!!(J+m-1)!!}{(J+m)!!(J-m)!!} \tag{2.30}$$

$$I_{J+m} = \begin{cases} 0, & J+m \ \text{ odd} \\ 1, & J+m \ \text{ even} \end{cases} \ .$$

With the previous definitions, the one-step surface response functions are given as $R^{\rm surf}_\alpha(q,\omega) = -{\rm Im} \sum_J (2J+1) \Pi^{\rm surf}_J(q,q;\omega)/4\pi^2$ and the double differential cross section turns out to be

$$\left.\frac{d^2\sigma}{d\Omega d\epsilon'}\right|_{\text{1-step}} = \sum_\alpha |f_\alpha(q)|^2 R^{\rm surf}_\alpha(q,\omega) \ , \tag{2.31}$$

to be compared with the effective number approximation, which reads

$$\left.\frac{d^2\sigma}{d\Omega d\epsilon'}\right|_{\text{1-step}} = N_{\text{eff}} \sum_\alpha |f_\alpha(q)|^2 R_\alpha(q,\omega) \ . \tag{2.32}$$

Multiple scattering inelastic contributions can, in principle, be incorporated along the same lines. Since in the kinematic regions of interest they turn out to be much smaller than the one-step terms, it is not worth going through a very complex formalism and one can safely stick to the effective number approximation. In this case, the two-step contribution is proportional to the convolution of two one-step response functions [17]. By summing over all the possible channels and using free one-step response functions, one can define the two-step response as

$$\begin{aligned} R^{(2)}(q,\omega) = \frac{\mathcal{D}_2}{k^2}\frac{1}{\sum_{ST}|f_{ST}(q)|^2}\int d\boldsymbol{q}' \int_0^\omega d\omega' \\ \left\{ \sum_{ST} |f_{ST}(q')|^2 R^{(0)}(q',\omega') \sum_{ST} |f_{ST}(|\boldsymbol{q}-\boldsymbol{q}'|)|^2 R^{(0)}(|\boldsymbol{q}-\boldsymbol{q}'|,\omega-\omega') \right. \\ \left. +2\sum_{S} |f_{S1}(q')|^2 R^{(0)}(q',\omega') \sum_{S} |f_{S1}(|\boldsymbol{q}-\boldsymbol{q}'|)|^2 R^{(0)}(|\boldsymbol{q}-\boldsymbol{q}'|,\omega-\omega') \right\} \ , \end{aligned} \tag{2.33}$$

where k is the momentum of the projectile, f_{ST} the KN amplitude in the S,T channel and

$$\mathcal{D}_2 = \frac{1}{2}\int d\boldsymbol{b}\, T^2(b) e^{-\widetilde{\sigma}_{\text{tot}} T(b)} \tag{2.34}$$

is proportional to the effective number of pairs participating in the double scattering.

The full quasielastic K^+-nucleus cross section discussed in Sec. III is given by the sum of one- and two-step terms:

$$\frac{d^2\sigma}{d\Omega d\epsilon'} = \sum_\alpha |f_\alpha(q)|^2 \left[R_\alpha^{\text{surf}}(q,\omega) + R^{(2)}(q,\omega) \right] \ . \tag{2.35}$$

We conclude this Section with a few remarks about the elementary K^+N amplitudes employed in the calculations. The amplitude for elastic K^+N scattering can be written as $f^{(s)} + f^{(v)}\tau_3$, with $f^{(i)} = g^{(i)} + i\boldsymbol{\sigma}\cdot\hat{\boldsymbol{n}}\, h^{(i)}$, $\hat{\boldsymbol{n}}$ being a unit vector normal to the scattering plane. In Fig. 5 one can see the amplitudes as a function of the momentum transfer for $k = 705$ MeV/c [18,19]: The dominant channel is clearly the scalar-isoscalar one.

Some care should be taken in the choice of the reference frame where the K^+N amplitudes are evaluated. In order to be able to factorize the two-body amplitude out of the nuclear response functions, an "optimal" choice of the reference frame has to be done [20,21]: The optimal momentum of the struck nucleon turns out to be

$$\boldsymbol{p}_{\text{opt}} = -\frac{\boldsymbol{q}}{2}\left(1 - \frac{\omega}{q}\sqrt{1+\frac{4m_N^2}{q^2-\omega^2}}\right) \ , \tag{2.36}$$

such as to reduce to zero at the QEP and to the Breit frame value at $\omega = 0$.

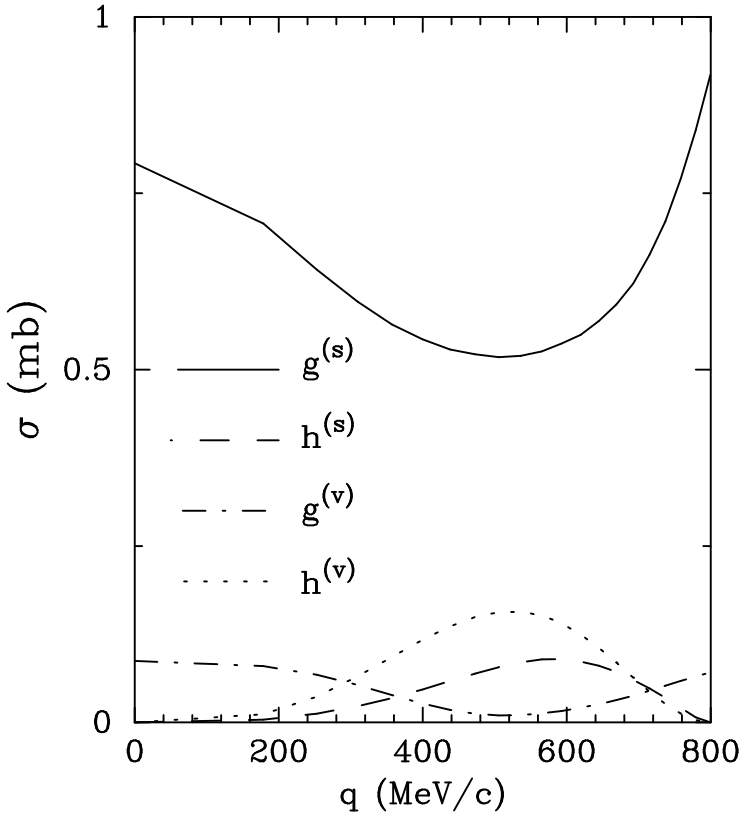

FIG. 5. Center-of-mass K^+N squared amplitudes corresponding to a K^+ laboratory momentum $k = 705$ MeV/c.

The most relevant consequence of this choice of frame is that the elementary projectile-nucleon amplitudes should be evaluated at an effective laboratory kinetic energy defined by

$$T_L^{\rm eff} = \frac{E_k E_{\rm opt} - \boldsymbol{k}\cdot\boldsymbol{p}_{\rm opt} - m_p m_N}{m_N} \ , \tag{2.37}$$

m_p and k being the projectile mass and momentum, respectively. This introduces a dependence on ω of the amplitudes entering in the evaluation of the quasielastic cross section, which can be important if the former are strongly energy dependent: At the kinematics of relevance to us, the effective K^+ momentum varies roughly in the range $500 \div 800$ MeV/c, where the amplitudes change sufficiently slowly to make the effects not at all dramatic.

III. RESULTS

Let us start by briefly discussing the relativistic kinematical effects, introduced at the end of Sec. II A. In Fig. 6 one can see the RPA scalar-isoscalar response of ^{12}C to K^+ probes in the non-relativistic case compared to the response function where the relativistic dispersion relation has been accounted for. As expected, the effect is negligible at the lowest

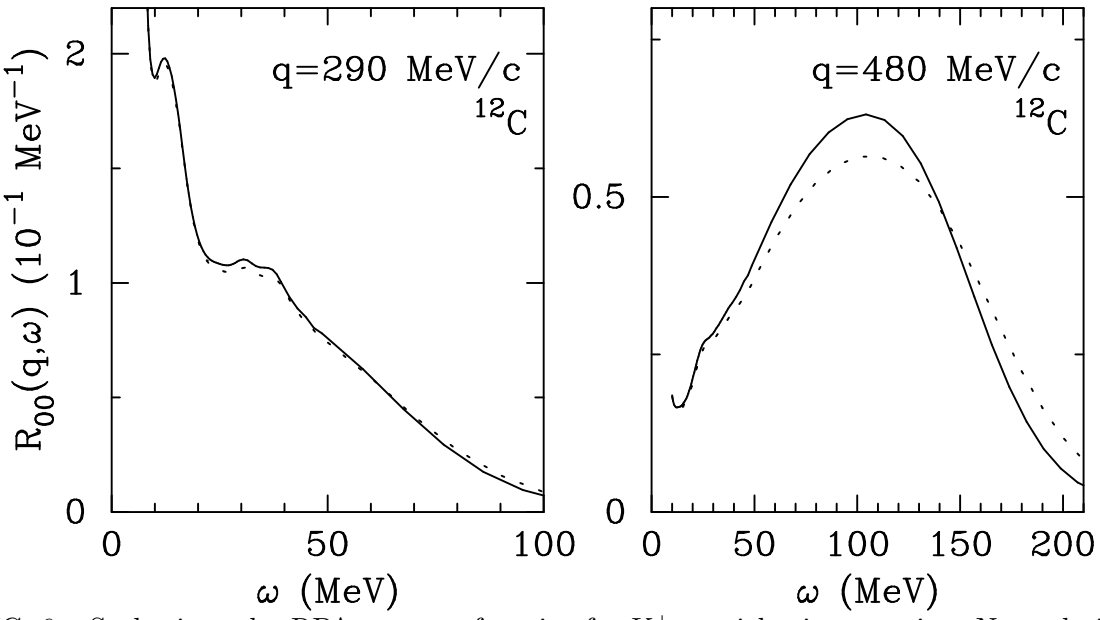

FIG. 6. Scalar-isoscalar RPA response function for K^+ quasielastic scattering: Non-relativistic (dotted) and with the kinematical relativistic corrections discussed in the text (solid).

momentum transfer (q = 290 MeV/c), whereas at higher momenta (q = 480 MeV/c) it produces a moderate shrink of the response at the right of the QEP, compensated by an enhancement ($\sim 10\%$) at the peak position.

Next, we would like to discuss the uncertainties connected to the choice of the effective ph interaction for quasielastic calculations. The knowledge of the latter suffers, in general, from many shortcomings: When it is theoretically calculated, — as the one we employ here (see Sec. II C), — sources of uncertainties arise because of the specific many-body scheme which has been adopted, from relativistic effects (see Ref. [22] for an effective interaction along the lines of Ref. [13], but in a relativistic context) and from the approximations made in the actual calculations or in extrapolating to the ph kinematical regime (see Sec. II C); when the effective interaction is just fitted to phenomenological properties, it can suffer from ambiguities in the parameterization (many sets of parameters reproducing the same body of data) and from the limited range of momenta which is covered (see, for instance, Ref. [14] for a phenomenological density-dependent interaction expressed in terms of Migdal-Landau parameters at $q \approx 0$).

On the other hand, one can of course reverse the argument and use the quasielastic studies to gain insight into the effective ph interaction at momentum transfers of a few hundreds MeV. One obvious difficulty in this case is related to the fact that it is not always possible to disentangle the various spin-isospin channels: The only reaction for which this has been achieved is the $(\vec{p},\vec{n})$ charge-exchange one, where the separated isovector spin-longitudinal and spin-transverse responses have been extracted [23]. However, the strong interaction of protons with nuclei constrains that reaction to the low density peripheral region of the nucleus, making it little sensitive to RPA effects; moreover, while the spin-longitudinal channel can be well described, the transverse one shows much more strength than expected

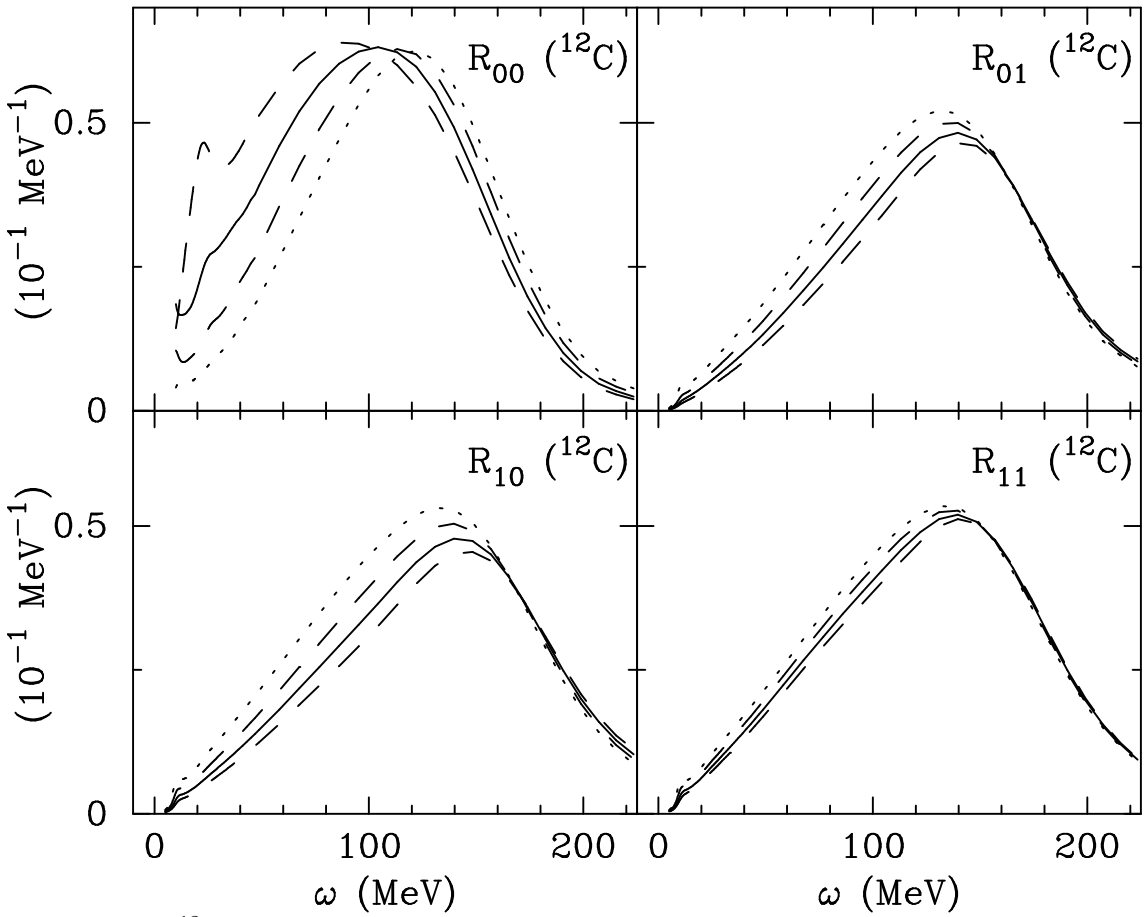

FIG. 7. K^+-^{12}C quasielastic response functions R_{ST} $(S, T = 0, 1)$ at $q = 480$ MeV/c. The dotted line represents the uncorrelated case; the solid line the RPA responses corresponding to the interaction of Sec. II C; the dashed lines the RPA responses with the same interaction scaled by $\pm 50\%$.

[6]. In this regard, the K^+-nucleus reaction is much more promising for two reasons: First of all, the small K^+N cross section makes the kaon enter inside the nucleus much more deeply than protons or pions, in turn implying stronger collective effects; secondly, as seen in Fig. 5, the scalar-isoscalar channel is largely dominant, making this reaction a "quasipure" probe of the $S = T = 0$ mode.

Whatever be the attitude towards this problem, we believe it is useful to gain some feeling about the sensitivity of the collective effects to the input effective potential. For this purpose, we display in Fig. 7, for the four spin-isospin channels, the surface RPA response functions at $q = 480$ MeV/c, calculated with the ph interaction discussed in Sec. II C, comparing them to the RPA responses calculated with the same interaction scaled by $\pm 50\%$. This amount for the rescaling is not an estimate of the theoretical or phenomenological uncertainty of the ph interaction; however, concerning the scalar-isoscalar channel, there are reasons to believe that the G-matrix estimate of Ref. [13] gives too much attraction: As discussed by the authors, the extracted f_0 Landau parameter makes nuclear matter unstable, a shortcoming

that can be cured by higher order contributions[1]. Thus, while the case with the interaction increased by 50% is taken mainly for illustrative purposes, the case with a weaker interaction is somewhat more realistic.

By inspecting Fig. 7 one can note the following:

i) the dependence of the responses on the potential is somehow desensitized by the RPA chain: For the $S = T = 0$ mode the variation of the response function at the left of the QEP is typically about $20 \div 30\%$, apart from the very low energy region ($\omega \lesssim 30$ MeV), where it grows up to $\sim 50\%$; for the other modes, still at the left of the QEP, the variation is always much smaller, say $\lesssim 5 \div 10\%$;

ii) at the right of the QEP the effect of correlations is much smaller, being limited to a few per cent for the $S = T = 0$ mode and to practically nothing for the other modes;

iii) the relatively weak sensitivity of the isovector and spin channels to variations of the input potential makes the small ($10 \div 20\%$) contamination from these modes in the K^+-nucleus cross section rather stable with respect to uncertainties due to correlations, enhancing the argument in favour of this reaction as a probe of the scalar-isoscalar channel.

The results if Fig. 7 are given for $q = 480$ MeV/c: Similar considerations apply also to the lowest momenta.

In Fig. 8 one can see the data for the quasielastic K^+-C cross section [1,2] compared to our calculations. In the theoretical cross sections, besides the case with free response functions (dotted), there are included the nuclear responses corresponding to the interaction of Sec. II C (solid) and to a reduction of 50% of the same interaction (dashed); the curves include the two-step contribution, which is also shown separately (dot-dashed).

From inspection of the figure, one sees that the strength of the cross sections on the right hand side of the QEP is well reproduced by both the correlated and the free responses (apart from the very high energy tail) at all the momentum transfers; however, at the lowest momenta the data show a clear distortion of the typical quasielastic shape, which is not compatible with the uncorrelated cross sections.

The experimental energy resolution is not sufficient to cut out the elastic scattering contribution; moreover, low-lying discrete nuclear excitations are much affected by the detail of the nuclear model (such as shell model parameters and spreading width). If, for these reasons, one excludes the very low energy tail (say, $\omega \lesssim 15$ MeV) it appears that the model with a weaker ph interaction gives a remarkably good description of the data at $q = 290$ and 390 MeV/c.

At the highest momentum, the elastic contamination and the discrete excitations have been washed out; the interaction in both the correlated models is sufficiently weak to cause little distortion of the quasifree shape, but the low energy part of the spectrum seems again to favour the model with the weaker ph interaction.

It is worth noticing the smallness of the two-step contribution, which is at most a few per cent of the one-step term at $q = 480$ MeV/c: This can be contrasted, for instance, to

---

[1] Also relativistic effects give rise to a weaker attraction: In Ref. [22] the strength in the $S = T = 0$ channel has been shown to be reduced by nearly a factor 1/2 at $q = 0$; however, in the range of momenta of interest to us, the relativistic and non-relativistic G-matrices appear to be comparable.

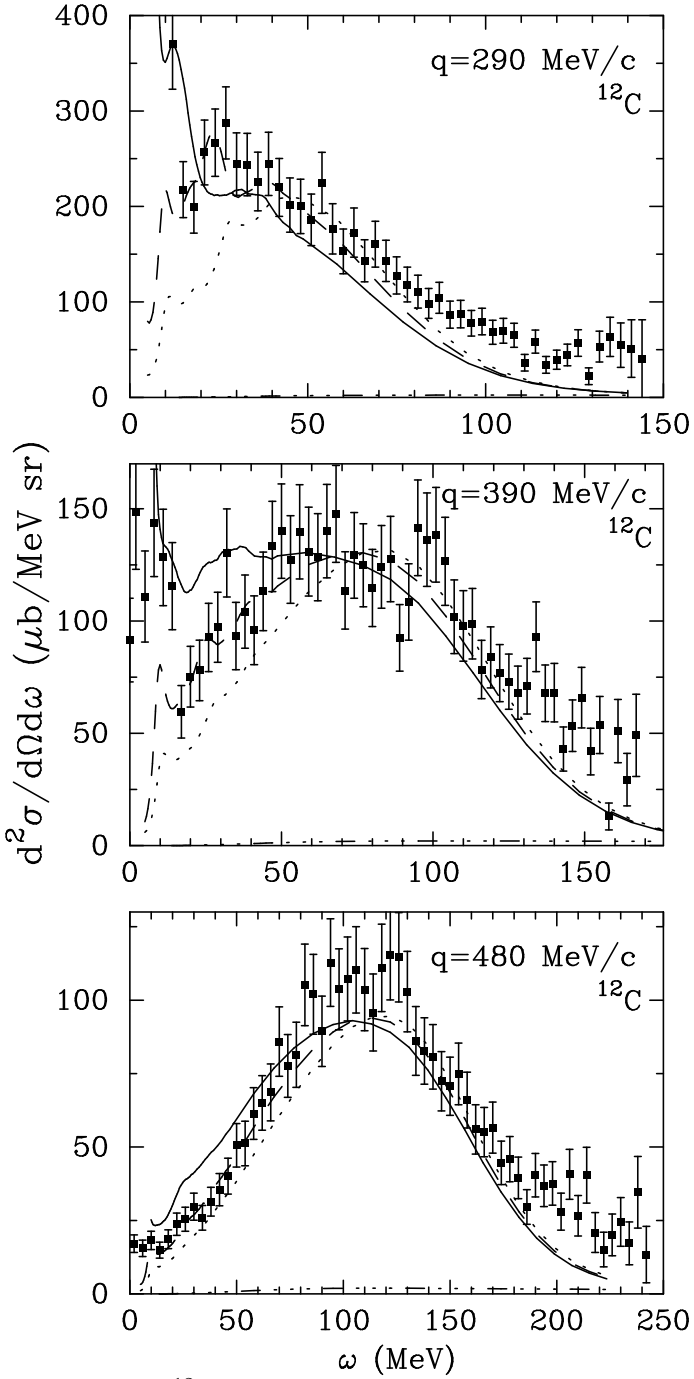

FIG. 8. Cross section for K^+-^{12}C quasielastic scattering: Free response (dotted), RPA with the interaction of Sec. II C (solid); RPA with the same interaction reduced by 50% (dashed). In all the cases, the two-step contribution has been added and it is also shown separately (dot-dashed).

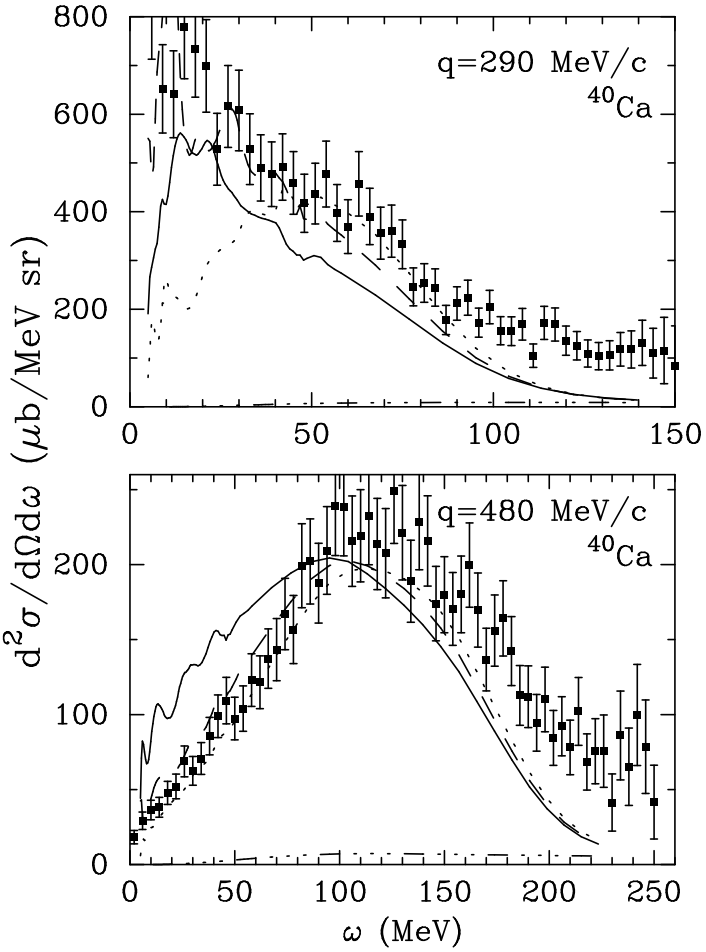

FIG. 9. As in Fig. 8, but for ^{40}Ca.

the isovector spin-transverse response to 500 MeV protons, where one finds, at $q \cong 500$ MeV/c, a sizeable $20 \div 30\%$ contribution from two-step processes [6]. Protons of 500 MeV of kinetic energy have a squared momentum which is roughly twice the one of 700 MeV/c kaons; furthermore, the two-step factor $\mathcal{D}_2$ of Eq. (2.33) and (2.34) is larger by roughly a factor two for the kaon reaction, — because of the smaller probe-nucleon total cross section $\widetilde{\sigma}_{\rm tot}$, — but this is compensated by the factor two arising from the two possible orderings of the charge-exchange reaction (see formula (8) of Ref. [6]). Hence, apart from a factor 2 in the coefficient, the relative weight of the two-step term in the two reactions has to be driven by the elementary amplitudes entering (2.33) (the response functions being in all the cases the free ones), that is by the factor $|f_{00}(|\boldsymbol{q}-\boldsymbol{q}'|)|^2|f_{00}(q')|^2/|f_{00}(q)|^2$ in (2.33) (since the scalar-isoscalar channel is dominant) and by the factor $|f_{00}^{NN}(|\boldsymbol{q}-\boldsymbol{q}'|)|^2|f_T^{NN}(q')|^2/|f_T^{NN}(q)|^2$ in the analogous expression for the (p,n) reaction, $\boldsymbol{q}$ being the external momentum and $\boldsymbol{q}'$ the integration variable, whereas f_T^{NN} and f_{00}^{NN} are the isovector spin-transverse and the scalar-isoscalar NN amplitudes, respectively.

The different size of the two-step contributions is indeed determined by the different strength and the different momentum behaviour of the above amplitudes: In the kaon case,

the scalar-isoscalar amplitude has little momentum dependence, so that $|f_{00}(q')|^2/|f_{00}(q)|^2$ is roughly between one and two, while the remaining squared amplitude is on average ~ 1.5 mb (in the laboratory); on the other hand, for the (p,n) reaction at $q \cong 500$ MeV/c, the ratio $|f_T^{NN}(q')|^2/|f_T^{NN}(q)|^2$ is typically in the range $4 \div 8$, whereas the remaining amplitude gives contributions mainly in the range from 10 to 22 mb. In qualitative words, we can say that because the NN cross section is relatively forward peaked, — unlike the K^+N one, — a double scattering in which the momentum transfer q is shared by the two nucleons is favored in the NN case with respect to the K^+N one.

Finally, we display also the available data for Ca at $q = 290$ and 480 MeV/c (Fig. 9). To these figures one can apply the same considerations made for the carbon data, although the preference for the weaker ph effective potential is even more clear now, since in heavier nuclei collective effects tend to be stronger. Indeed, the sensitivity of the response functions to variations in the input potential is a little more pronounced in ^{40}Ca than in ^{12}C, being about $25 \div 35\%$ for a 50% change of the potential in the $S = T = 0$ channel, to be compared to the $20 \div 30\%$ sensitivity found in ^{12}C (see the discussion of Fig. 7). Also the two-step contribution is, as expected, larger in ^{40}Ca than in ^{12}C.

IV. CONCLUSIONS

From the discussion in the previous Section, it appears that the model presented here gives a good description of the quasielastic K^+ data, the main uncertainty being related to the strength of the effective ph interaction in the scalar-isoscalar channel. A good description of the data was achieved by using the interaction of Ref. [13] quenched by 50%. It was shown that the use of this interaction with the full strength led to results in clear contradiction with the data. Indeed, there are theoretical indications that the strength of this interaction in the scalar-isoscalar channel should be reduced. On the other hand, from Figs. 8 and 9 one can see that the K^+ data can be used to constrain the strength of the ph potential for the $S = T = 0$ mode.

There are, however, two issues that need to be commented upon, namely the reported high experimental values for the effective number of nucleons $N_{\rm eff}$ [1,2] (see the Introduction) and the comparison with the available calculations for this reaction that employ relativistic dynamical models [1,2,16].

Concerning the first point, it might appear curious that the "experimental" value for $N_{\rm eff}$ quoted in Refs. [1,2] be $\sim 30\%$ higher than the one calculated in the Glauber model, since we have seen that the latter gives a nice estimate of the quasielastic cross sections. A source of error may of course be given by the use of the effective number approximation (2.32); however, we believe that the main reason for the overestimate of $N_{\rm eff}$ lies in the way followed to extract the effective number from the data [2]. Indeed, $N_{\rm eff}$ has been obtained by integrating the quasielastic data over the whole range of transferred energies: In order to do this, the data have been fitted with Gaussian distributions and, although a subtraction of the elastic scattering and low energy excited levels contributions has been attempted, *no subtraction for any high energy background has been included*. From Figs. 8 and 9 it appears that the very high energy tail of the cross sections is underestimated by the calculations, both for the free and the correlated models (remember, from the discussion of Sec. III, that while

RPA correlations sizably affect the low energy side of the QEP, they have little influence on the high energy part). The data actually seem to show some structure beyond the ph response region: In the case of quasifree electron scattering, the strength in this region is attributed to effects beyond RPA (such as meson-exchange currents or 2p–2h excitations). Note also that a simple, "straight line", estimate of the background brings the value of $N_{\rm eff}$ in close agreement with the Glauber estimate [24].

Meson-exchange currents effects tied to the interaction of the kaon with the nuclear pion cloud have been evaluated in Refs. [25,26] and found to lead to small corrections to the K^+-nucleus total cross section. The consideration of contact terms using chiral Lagrangians makes the corrections even smaller [27], so that this source of corrections cannot account for the strength at large values of ω. On the other hand, the tail of the Δ excitation reaches this region, since the Δ acquires a finite width, even below the pion production threshold, due to the $\Delta N \to NN$ reaction in the nucleus. Hence, the channel of kaon induced Δ excitation in nuclei should become a target of both theoretical and experimental investigation in order to further clarify these issues.

Concerning the calculations with relativistic models of Refs. [1,2,16], it is obviously difficult to make a comparison with our results, since in those papers the RPA response functions (calculated in a variety of models) have been multiplied by the "experimental" $N_{\rm eff}$, so that their strength is just fitted to the data (of course, the use of the calculated value for $N_{\rm eff}$ would result in a general underestimate of the cross sections). However, it should be noticed that the relativistic RPA isoscalar response is *quenched*, in contrast to our non-relativistic RPA response, which is mainly shifted to the left and enhanced at very low energies. Then, it is clear that this quenching has to be compensated by a higher $N_{\rm eff}$. Also to be noticed is the fact that the relativistic RPA calculations are able to describe (albeit through a fit of the total cross section) only the data at high momentum transfers. At $q = 290$ MeV/c, the large enhancement in the cross section visible at moderate energy transfers ($15 \lesssim \omega \lesssim 40$) is clearly not predicted, even in a finite nucleus calculation [1], in contrast to our non-relativistic results.

Of course, before drawing more firm conclusions one should test the model also against the (e, e') data and calculations in this direction are in progress. In this connection, it is interesting to note that a recent reanalysis of the (e, e') world data [28] seems to rule out the long-standing problem of the missing strength in the charge channel, which had been interpreted in terms of a quenching of the charge response.

ACKNOWLEDGMENTS

We would like to acknowledge R. J. Peterson for sending us detailed information on the experiments. This work has been supported by the program of Human Capital and Mobility of the EU, contract n. CHRX–CT 93–0323, and by CICYT, contract n. AEN 96–1719.

REFERENCES

[1] C. M. Kormanyos *et al.*, Phys. Rev. Lett. **71**, 2571 (1993).
[2] C. M. Kormanyos *et al.*, Phys. Rev. C **51**, 669 (1995).
[3] D. Marlow *et al.*, Phys. Rev. C **25**, 2619 (1982).
[4] P. B. Siegel, W. B. Kaufman, and W. R. Gibbs, Phys. Rev. C **30**, 1256 (1984).
[5] A. De Pace and M. Viviani, Phys. Rev. C **48**, 2931 (1993).
[6] A. De Pace, Phys. Rev. Lett. **75**, 29 (1995).
[7] A. L. Fetter and J. D. Walecka, *Quantum Theory of Many-Particle Systems* (McGraw-Hill, New York, 1971).
[8] R. D. Smith and J. Wambach, Phys. Rev. C **38**, 100 (1988).
[9] C. Mahaux and H. Ngô, Phys. Lett. **100B**, 285 (1981).
[10] W. M. Alberico, M. B. Barbaro, A. De Pace, T. W. Donnelly, and A. Molinari, Nucl. Phys. **A563**, 605 (1993).
[11] J. E. Amaro, J. A. Caballero, T. W. Donnelly, A. M. Lallena, E. Moya de Guerra, and J. M. Udías, Nucl. Phys. **A602**, 263 (1996).
[12] W. M. Alberico, A. De Pace, and A. Molinari, Phys. Rev. C **31**, 2007 (1985).
[13] K. Nakayama, S. Krewald, J. Speth, and W. G. Love, Nucl. Phys. **A431**, 419 (1984).
[14] J. Speth, E. Werner, and W. Wild, Phys. Reports **33**, 127 (1977).
[15] R. J. Glauber, in *Lectures in Theoretical Physics*, edited by W. Brittin *et al.* (Interscience Publishers, New York, 1959), Vol. 1.
[16] J. Piekarewicz and J. R. Shepard, Phys. Rev. C **51**, 806 (1995).
[17] R. D. Smith and J. Wambach, Phys. Rev. C **36**, 2704 (1987).
[18] R. A. Arndt, L. D. Roper, and P. H. Steinberg, Phys. Rev. D **18**, 3278 (1978); R. A. Arndt and L. D. Roper, *ibid* **31**, 2230 (1985).
[19] B. Martin, Nucl. Phys. **B94**, 413 (1975).
[20] S. A. Gurvitz, Phys. Rev. C **33**, 422 (1986).
[21] R. D. Smith, in *Proceedings of the International Conference on Spin Observables of Nuclear Probes*, Telluride, Colorado, 1988, edited by C.J. Horowitz, C.D. Goodman and G. Walker, (Plenum, New York, 1989),p. 15.
[22] K. Nakayama, S. Drozdz, S. Krewald, and J. Speth, Nucl. Phys. **A470**, 573 (1987).
[23] T. N. Taddeucci *et al.*, Phys. Rev. Lett. **73**, 3516 (1994).
[24] C. M. Kormanyos and R. J. Peterson, Nucl. Phys. **A585**, 113c (1995).
[25] M. F. Jiang and D. S. Koltun, Phys. Rev. C **46**, 2462 (1992).
[26] C. García-Recio, J. Nieves, and E. Oset, Phys. Rev. C **51**, 237 (1995).
[27] Ulf-G. Meissner, E. Oset, and A. Pich, Phys. Lett. **B353**, 161 (1995).
[28] J. Jourdan, Nucl. Phys. **A603**, 117 (1996).